BEAM COUPLING IMPEDANCE MEASUREMENTS OF THE DAΦNE VACUUM CHAMBER COMPONENTS

F. Marcellini, D. Alesini, R. Boni, A. Gallo, A. Ghigo, M. Serio, M. Zobov

LNF-INFN, Frascati, Italy

Abstract

Multibunch operation in high current storage rings like DAΦNE can be seriously limited by coupled bunch oscillations driven by resonant e.m. fields trapped somewhere along the vacuum chamber. The design of each vacuum chamber component aims to keep the beam coupling impedance below the values for which multibunch instabilities can be controlled by feedback systems. The impedance of some of the most critical devices has been measured and a summary of the obtained results is presented.

1 INTRODUCTION

The DAΦNE Φ-factory is a double ring e^+e^- collider designed for a target luminosity of $\approx 5\ 10^{32}\ cm^{-2}\ s^{-1}$ at the c.m. energy of 1.02 GeV. To get the required luminosity both single and multibunch high current values (≈5 A over 120 bunches in each ring) are foreseen.

A charged particle beam is a source of e.m. fields that interact with the surrounding vacuum chamber, where image currents are induced. As a consequence, beam power is dissipated in the pipe walls because of their finite conductivity, heating and sometimes damaging the vacuum chamber components.

Moreover, high order modes (HOM) in the RF cavities and resonant modes, trapped where any discontinuities of the pipe cross-section occur, could drive coupled bunch instabilities and limit the ultimate luminosity.

The e.m. interaction between the beam and its surroundings can be described, in time domain, by means of the wake function or by its Fourier transform, the beam coupling impedance, in frequency domain.

Careful estimates and measurements of beam impedance are necessary in order to guarantee the design performances.

In this paper we describe the methods used for DAΦNE impedance measurements and summarize the results obtained for the most critical vacuum chamber components.

2 COAXIAL WIRE METHOD TECHNIQUE

The technique used for impedance measurements is based on the wire method described in literature (see for example Refs. [1], [2]). Frequency domain measurement application as well as some intrinsic limit of the method are reported in the following.

2.1 Longitudinal coupling impedance

In the longitudinal case, the experimental set up is schematically sketched in Fig. 1. The basic idea is to force a current along a coaxial conductor placed inside the structure one wants to measure (Device Under Test, DUT), in order to create the same field configuration of a centered beam (see Fig. 2).

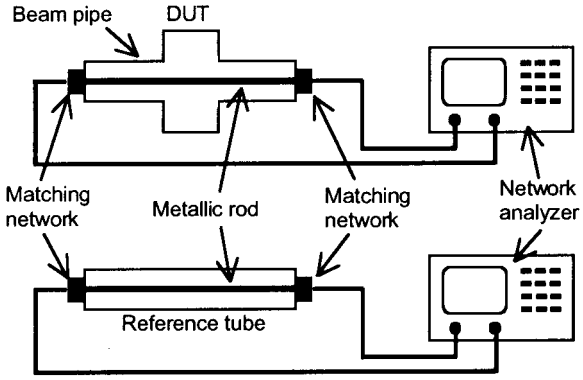

Figure 1: Sketch of the experimental set up used for longitudinal impedance measurements.

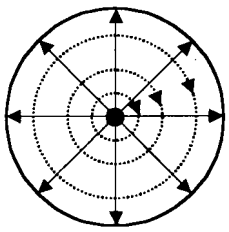

Figure 2: Transverse e.m. field distribution (TEM mode) generated by the beam pipe centered conductor (E-field: solid line, H-field: dotted line).

The device frequency response is measured by means of a vector network analyzer; the whole beam spectrum can be covered by sweeping the signal frequency.

The main problem one has to cope with is the isolation of the DUT response from any other parasitic contribution. Two resistive networks are used at each transition between the wired beam pipe coaxial line and the connecting cables in order to match their different characteristic impedance. This solution limits the reliability of the measurement to relatively low frequencies, but it is quite easy to realize and can be readapted to different pipe cross-section simply by varying the resistance values.

At high frequency: a) the parasitic reactance of the matching resistors change their impedance with frequency; b) resistive matching is ineffective for the higher order coaxial modes. For this reason, above the TE_{11} frequency cut-off, coaxial resonances of TE_{11n} (n = 1, 2,…) type are usually measured and their discrimination respect to the DUT resonances is often not an easy task.

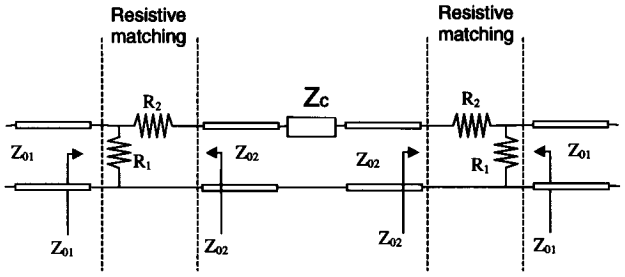

Figure 3: Equivalent circuit of impedance measurements.

Usually, in order to subtract all the spurious terms from the response obtained from DUT measurement, a reference tube (i.e. a structure where the DUT is replaced by a straight section of the beam pipe) measurement is performed . Nevertheless, this expedient is often not sufficient to clearly discriminate actual DUT resonances from TE_{11n} resonances, because of their different frequencies due to coax line field perturbation introduced by the DUT.

The measurement equivalent circuit is shown in Fig. 3. The cables connecting the structure under measurement to the N.A. are represented by transmission lines having Z_{01} characteristic impedance, while Z_{02} is the characteristic impedance of the coaxial line formed by the beam pipe and the inner conductive rod. Matching between the two transmission lines is realized choosing:

$$R_1 = Z_{01}\sqrt{\frac{Z_{02}}{Z_{02}-Z_{01}}} \text{ and } R_2 = \sqrt{Z_{02}\left(Z_{02}-Z_{01}\right)}.$$

The coupling impedance is approximated as a lumped element and its value can be obtained from:

$$Z_c = 2Z_{02}\left(\frac{S_{21ref}}{S_{21dut}}-1\right),$$

where S_{21} is the scattering matrix parameter measured as the N.A. output to input port signal ratio.

2.2 Transverse coupling impedance

The set up used for transverse measurements is shown in Fig. 4 and differs only because a pair of parallel wires is inserted into the structure and aligned on the horizontal (vertical) plane if horizontal (vertical) impedance has to be measured.

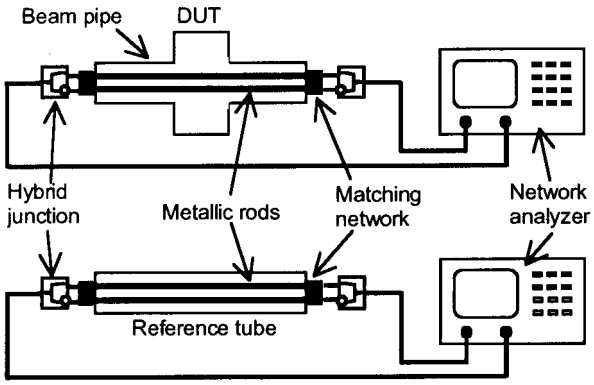

Figure 4: Sketch of the experimental set up used for transverse impedance measurements.

Using two 180° hybrid junctions as shown schematically in Fig. 4, two identical currents, but with opposite direction, flow along the wires, giving rise to the field configuration shown in Fig. 5.

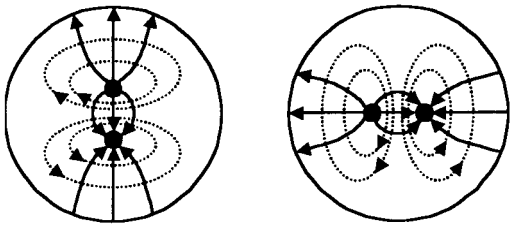

Figure 5: Transverse e.m. field distribution (TEM mode) generated by two parallel conductors in a beam pipe (E-field: solid line, H-field: dotted line).

In this case the beam coupling impedance is given by:

$$Z_c = Z_{02}\left(\frac{S_{21ref}}{S_{21dut}}-1\right),$$

being Z_{02} the characteristic impedance of the transmission line formed by a single wire and the pipe halved by an electric symmetry plane.

2.3 Transfer impedance

The same experimental set up described above for coupling impedance, can be used for transfer impedance measurements. When a device has some output port, it is possible to define the beam transfer impedance of that port

as $Z_t=V_i/I_b$, where V_i is the voltage induced on i-th port as effect of the beam-structure interaction and I_b is the beam current value.

The transfer impedance for port i is given by:

$$Z_t = \left| \frac{S_{i1dut}/S_{i1ref}}{S_{21dut}/S_{21ref}} \right| \sqrt{Z_0 Z_{02}} ,$$

being Z_0 the characteristic impedance of the transmission line related to the port. In the previous formula S_{i1ref} is just an ideal, not measurable quantity, but it is possible to assume $S_{i1ref} = \sqrt{S_{21ref}}$ if the two matching networks are considered identical.

3 IMPEDANCE MEASUREMENT RESULTS

Several devices or components of the DAΦNE vacuum chamber have been characterized by beam coupling and/or transfer impedance measurements. Measurement results have been often complemented by numerical ones obtained from a FEM analysis of the structure, performed by HFSS [3] and MAFIA [4] codes. In particular, ideal wire measurements (perfect matching conditions) have been, in some cases, simulated by HFSS.

A brief description of the obtained results is given in the following for the most critical components.

3.1 Bellows

The DAΦNE rings are equipped with 36 bellows for thermal expansion compensation. 20 of them (straight section bellows [5]) are located in the straight sections, while the remaining (arc section bellows [6]) are used to join the arcs to the straight sections.

In the latter, the discontinuity introduced by the bellows in the vacuum chamber section was initially shielded by two grids of thin, wave shaped, metallic strips.

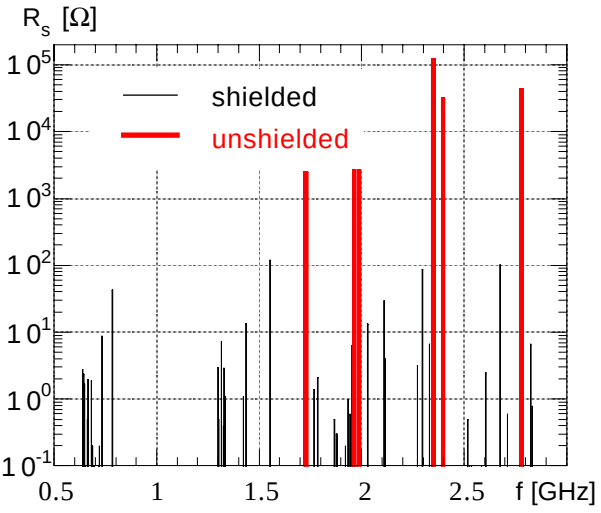

Figure 6: Measured impedance of the arc section bellows with and without the prototype shield inside.

As shown in Fig. 6, the screen successfully eliminates the bellows resonant modes, but introduces two kinds of new weaker resonances:

- HOMs trapped between the strips;
- coaxial cavity type modes (where the bellows chamber and the shield are the outer and the inner conductor respectively) that couple with the beam through a lateral slot left in the screen to let synchrotron radiation go out.

All of them have a wavelength $\lambda \approx 2l/n$ (n = 1, 2,...), being l the bellows length.

The shield was then modified introducing transverse ribs in order to shorten the resonator length (see Fig. 7). As a result, lower frequency modes disappear.

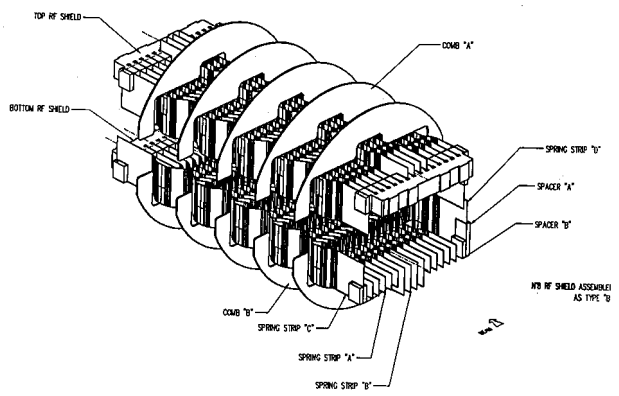

Figure 7: Sketch of the arc section bellows shield.

Moreover a solution with only one slot, on the side exposed to the synchrotron light, for the downstream bellows and no slots at all for the upstream ones, was finally adopted to limit the number of residual coaxial modes.

The resonances measured in both the cases are displayed in Fig. 8.

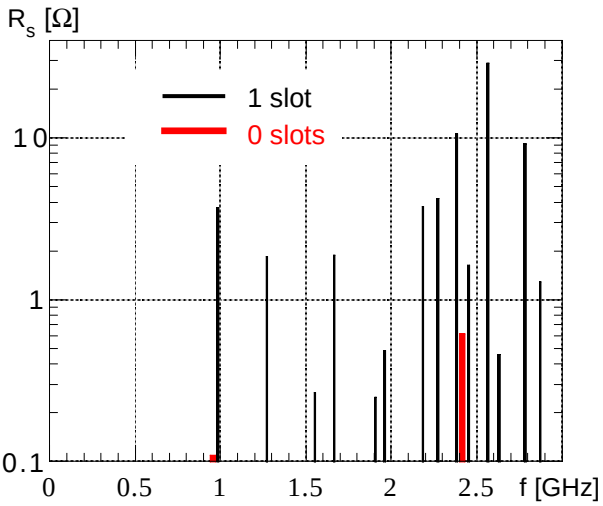

Figure 8: Measured impedance of the arc section bellows with the finally adopted shields.

A different solution has been chosen for the straight

section bellows, where the shield consists of a number of mini-bellows placed around the bellows gap, in such a way to fit the beam pipe shape. Since the wire method measurement (see Fig. 9) has shown no significant difference with respect to the reference tube frequency response up to 3.5 GHz, this structure results free of measurable longitudinal resonant modes.

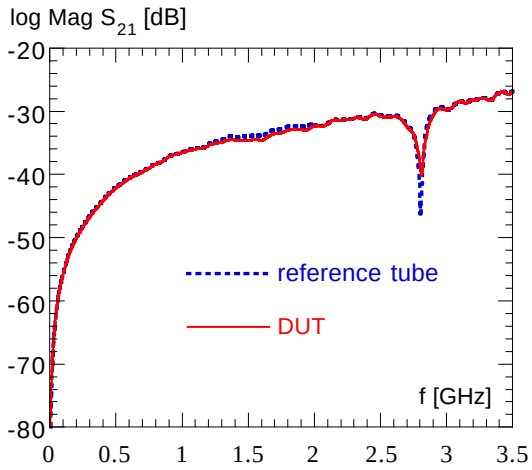

Figure 9: Frequency responses obtained in wire measurement of straight section bellows.

3.2 *Longitudinal feedback kicker*

The DAΦNE longitudinal kicker [7] consists of a pill-box cavity resonating at $13/4 \cdot f_{RF}$, strongly loaded by 6 special ridged waveguides in order to have the bandwidth required to cover the whole spectrum of possible coupled bunch mode frequencies and to get rid of higher order modes.

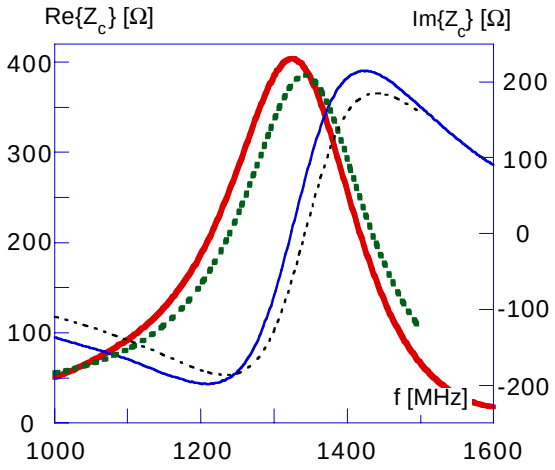

Figure 10: Coupling impedance of the longitudinal feedback kicker. (thick lines: resistive part of impedance, thin lines: reactive part; solid lines: wire measurements, dotted lines: HFSS wire method simulations).

Both wire method measurements and simulations have been performed for longitudinal impedance evaluation. Results are summarized in Fig. 10. Because of the strong field distortion due to the insertion of the wire into the structure, a frequency shift of the resonant peak occurs.

3.3 *Transverse feedback kicker*

The DAΦNE transverse kicker [8] is based on a strip-line pair design where each electrode forms a transmission line of 50Ω characteristic impedance with the vacuum pipe. Both ends of the electrodes are properly terminated through a transition to coaxial line. In spite of the tapered tank, used to reduce parasitic power losses and coupling impedance, two HOMs remain trapped in the structure. Their damping is provided by two loop couplers.

The beam coupling impedance and the transfer impedance of the kicker ports, obtained both from measurements and from e.m. simulations, are reported in graphs of Figs. 11 and 12.

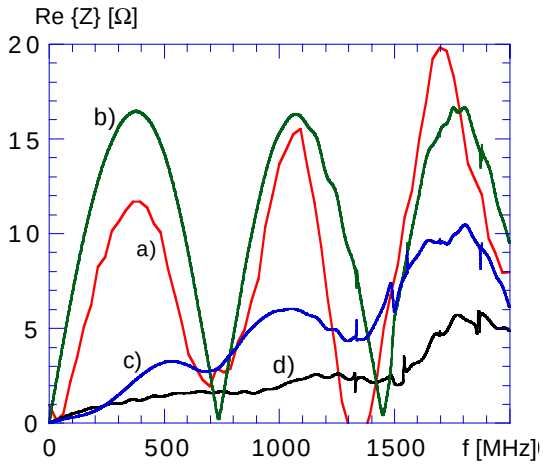

Figure 11: Transverse feedback kicker measurements: a) beam coupling impedance; b) upstream port transfer impedance; c) downstream port transfer impedance; d) loop transfer impedance.

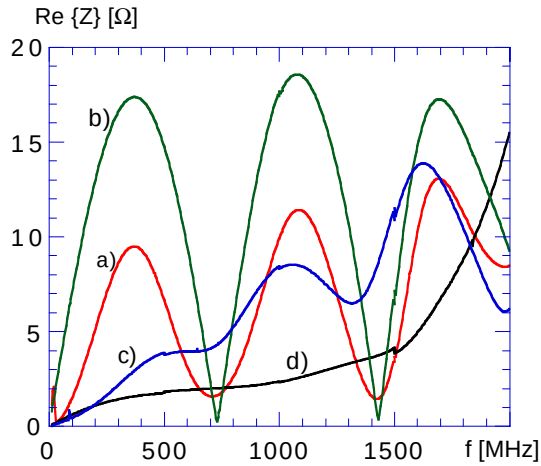

Figure 12: Transverse feedback kicker HFSS simulations: a) beam coupling impedance; b) upstream port transfer impedance; c) downstream port transfer impedance; d) loop transfer impedance.

3.4 RF cavity

The DAΦNE RF cavity [9], [10] is a single cell resonator attached to the beam pipe through two tapered sections where special loading waveguides are placed for HOM damping. Three further larger waveguides couple the lower frequency HOMs directly on the cavity body. The WGs cut-off frequency is higher than the fundamental mode frequency so that it remains almost unperturbed (Q value reduced by ~ 12%).

The cavity longitudinal impedance measurements have pointed out a general effective damping of the HOMs as qualitatively displayed in Fig. 13.

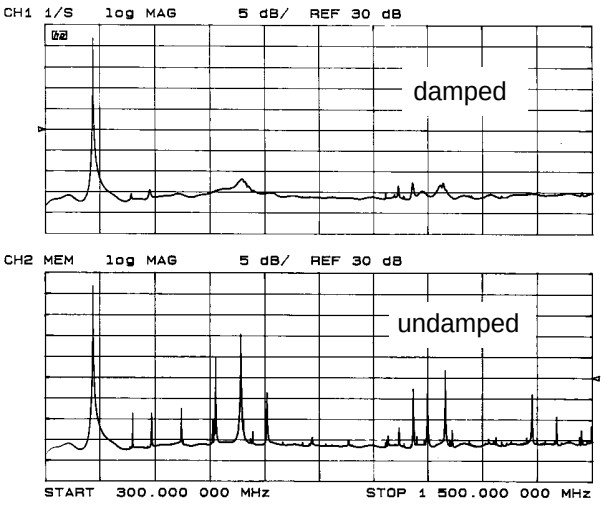

Figure 13: RF cavity longitudinal coupling impedance.

Since the WGs, the RF input coupler and the tuner break the 2-D symmetry of the original cell, also higher polarity transverse modes have some field component along the beam axis, that can be measured with longitudinal set up. For example, around 0.5 GHz, the first two dipolar modes are clearly recognizable.

Finally, the wire introduces a strong field perturbation of the fundamental mode, which results damped and shifted towards higher frequency, similarly as in the longitudinal kicker case.

3.5 Injection kicker

A schematic view of the injection kicker internal structure and its connections with external devices is given in Fig. 14.

The pulse generator current flows into the kicker inner conductors, giving rise to the deflecting e.m. field along the beam axis, then crosses a coaxial ferrite device (magnetic switch) used for signal ringing suppression.

Just before installation, longitudinal coupling impedance of the injection kicker has been measured.

As pointed out in Fig. 15, several high impedance HOMs trapped in the structure have been found.

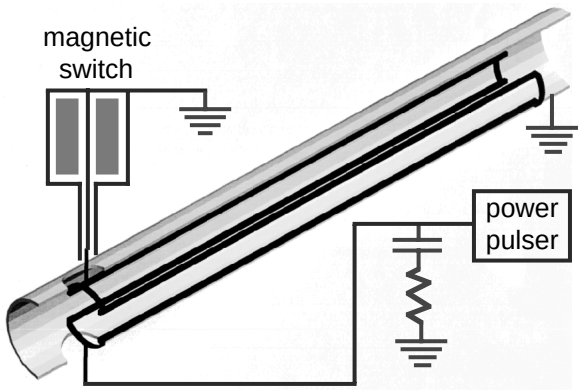

Figure 14: Schematic of injection kicker system.

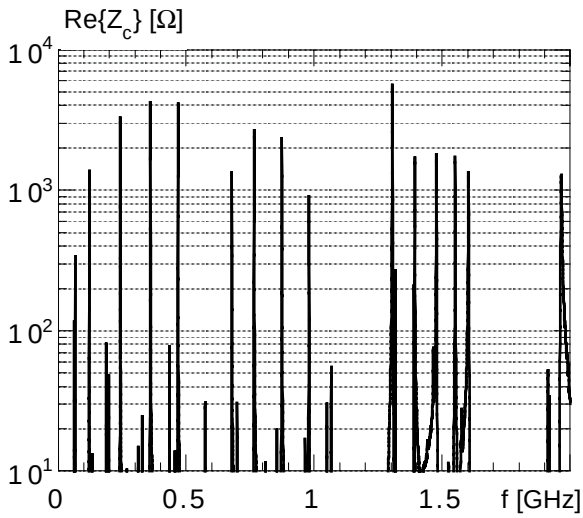

Figure 15: Longitudinal coupling impedance of the injection kicker structure only.

When the magnetic switch is connected to the kicker feedthrough, the resonances are partially damped, as consequence of the power dissipated in the ferrite. This could lead to overheating and damaging of the device.

As indicated in Fig. 14, an external HOM damping was attempted by the insertion of an RC high pass filter capable to dissipate the HOM power and to reject the low frequency signal from the pulse generator.

Unfortunately, this solution has resulted of little effectiveness for the higher frequency modes (see Fig. 16) and new kickers, provided with two HOM couplers inside, are presently under construction [11].

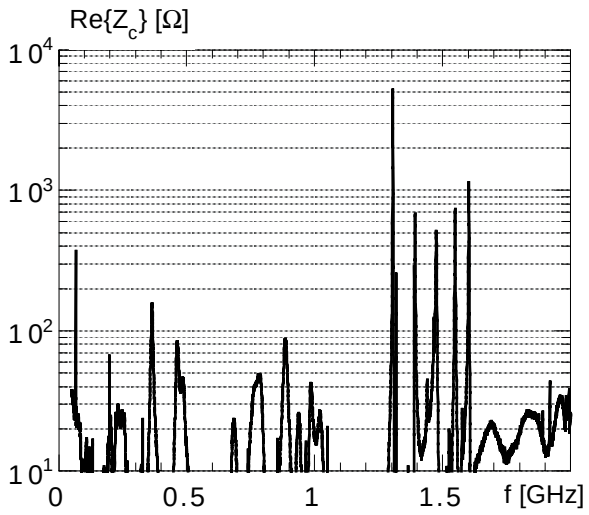

Figure 16: Longitudinal coupling impedance of the injection kicker with pulser, magnetic switch and RC filter connected.

3.6 Beam current monitors

The beam average current in DAΦNE is measured by a DC current transformer (DCCT) [12] placed outside the vacuum chamber, around a ceramic break of the aluminum pipe to avoid detection of parasitic wall currents. A conducting wire net is wrapped around the DCCT to restore the electrical continuity of the chamber. The structure is sketched in Fig. 17.

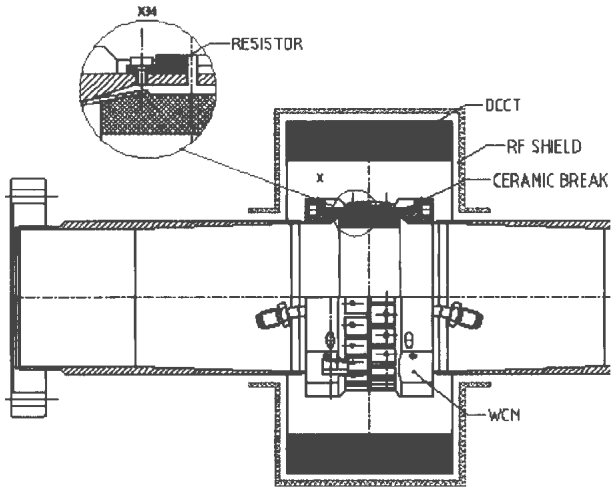

Figure 17: Schematic cut-view of the beam current monitors.

In this way, the beam generated e.m. fields propagate through the ceramic gap and can originate dangerous resonant modes inside the volume defined by the outer envelope.

Moreover, the DCCT ferrite core could suffer damages for overheating, as it partially absorbs the HOM fields (see Fig. 18).

HOMs are eliminated shunting the ceramic gap by means of 50 power resistors (50Ω each) uniformly welded around the pipe. In fact the resistors act as an effective shield for the higher frequency e.m. fields (resonances are no more measured), while almost the whole DC wall currents still pass through the low impedance (<<1Ω) external wire netting.

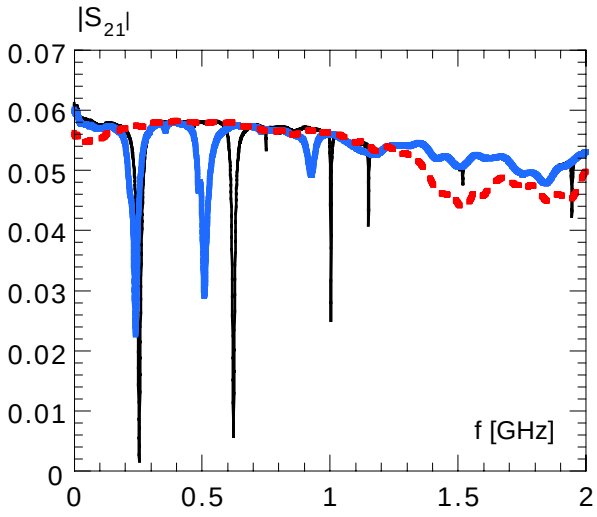

Figure 18: Wire measurement frequency response of the shielded ceramic break (thin line: outer shield without DCCT; thick line: outer shield with DCCT inside; dotted line: gap shielded by shunting resistors).

Finally, the voltage drop signal at the ends of the resistors can be used for beam current monitoring in the same way as in a wall current monitor (WCM).

3.7 Pick-up for the feedback systems

Three beam position monitors are used in the front-end section of longitudinal, horizontal and vertical feedback systems to detect the single bunch synchronous phase and transverse position offsets.

Each BPM consists of 4 electrodes [13] designed to have a flat frequency response on a bandwidth large enough to discriminate the signals induced by adjacent bunches. Further requirements have been the absence of any trapped HOM and a contribution to the machine coupling impedance as small as possible.

Analytical and numerical transfer impedance estimates, compared to wire method measurement are shown in Fig. 19.

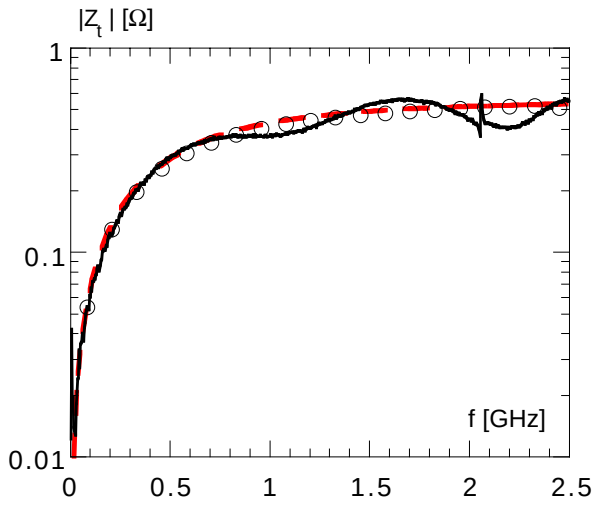

Figure 19: Transfer impedance of the feedback system pick-up (dotted line: analytical expression; circles: HFSS simulations; solid line: wire measurements).

3.8 Interaction region vacuum chamber

The KLOE detector beam pipe [14] has a bulb like shape centered at the interaction point. The spherical bump of the chamber is shielded by two half cylindrical, very thin (50 μm), metallic surfaces in order to avoid any electromagnetic discontinuity seen by the beam. For vacuum purposes, the shield has an equatorial slot where coupling of beam generated fields with the volume outside the screen may occur.

While no resonances have been measured below 2 GHz, in the frequency range between 2 and 3.1 GHz, 14 modes have been found, with impedance values from few ohms to some tens of ohm (see Fig. 20). Nevertheless, taking into account that TE_{11} frequency cut-off of the pipe is 2.004 GHz, they are likely to be TE_{11n} type coaxial line resonances. In fact, 12 TE_{11n} (n = 1, 2,..., 12) modes lies in the 2 ÷ 3.1 GHz frequency range and 7 of them appear from reference beam tube measurements. Moreover, for a given n it could be measured a double resonant peak for degeneration of TE_{11} polarization.

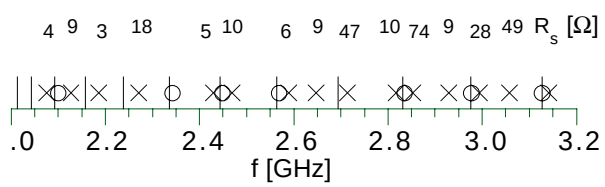

Figure 20: KLOE vacuum chamber coupling impedances (bars: calculated TE_{11n} resonances; circles: reference tube measurements; crosses: DUT measurements. Numbers refer to the measured DUT impedance values).

4 CONCLUSIONS

The vacuum chamber impedances obtained from simulations and measurements have been used to formulate the model impedance of the storage rings, in order to predict the bunch lengthening and single bunch thresholds. The measurements performed on the beam agree with the estimates obtained from the model [15].

REFERENCES

[1] M. Sands and J. Rees, " A Bench Measurement of the Energy Loss of a Stored Beam to a Cavity", SLAC-Note PEP-95, August 1974.

[2] H. Hahn and F. Pedersen, " On Coaxial Wire Measurement of the Longitudinal Coupling Impedance", BNL 50870, Particle Accelerators and High Voltage Machines TID-4500, April 1978.

[3] Hewlett Packard Co, "HP 85180A™ High Frequency Structure Simulator. User's Reference. Release 4.0", Hewlett Packard, 1996.

[4] R. Klatt et al. "MAFIA - A three-dimensional electromagnetic CAD system for magnets, RF structures and transient wake field calculations", SLAC report 303, 1986.

[5] G. O. Delle Monache et al. "Power Losses in the DAΦNE Bellows Shields", DAΦNE Technical Note G-43, Frascati, November 96.

[6] G.O. Delle Monache et al. "DAΦNE Shielded Bellows", Nuclear Instruments and Methods in Physics Research A 403 (1998), p 185.

[7] R. Boni et al., "A waveguide overloaded cavity as longitudinal kicker for the DAΦNE bunch-by-bunch feedback system", Particle Accelerators, Vol. 52, p. 95.

[8] R. Boni et al., "Longitudinal and Transverse Kickers for the Bunch-by-Bunch Feedback Systems of the Frascati Φ-Factory DAΦNE ", Proc. of Beam Instrumentation Workshop '96, Argonne, IL, USA, May '96, p. 381.

[9] S. Bartalucci et al. "Analysis of Methods for Controlling Multibunch Instabilities in DAΦNE", Particle Accelerators, Vol. 48, 4 (1995), p. 213.

[10] R. Boni et al., "A Broad Band Waveguide to Coaxial Transition for High Order Mode Damping in Particle Accelerator RF Cavities", Particle Accelerators, Vol. 45, 4 (1994), p. 195.

[11] D. Alesini et al. "DAΦNE injection kicker: electromagnetic analysis of trapped modes and damping antenna design", this Workshop.

[12] A. Ghigo et al., "DAΦNE Beam Instrumentation", AIP Conference Proceedings 451, Proc. of Beam Instrumentation Workshop '98, Stanford, CA,, May '98, p. 183.

[13] F. Marcellini et al. "DAΦNE Broad Band Button Electrodes", Nuclear Instr. Meth. in Phys. Res. A 402 (1998) p. 27.

[14] G. O. Delle Monache and G. Raffone "Be Chamber at KLOE I.P.: RF Shield Mechanical Design", DAΦNE Technical Note ME-6, Frascati, July "96.

[15] M. Zobov et al. "Bunch lengthening and Microwave Instability in the DAΦNE Positron Ring", DAΦNE Technical Note BM-3, Frascati, June "98.